Organic & Biomolecular Chemistry

PAPER

View Article Online
View Journal | View Issue

Check for updates

Cite this: *Org. Biomol. Chem.*, 2018, **16**, 8095

Immune responses against Lewis Y tumor-associated carbohydrate antigen displayed densely on self-assembling nanocarriers†

Yuji Yamazaki,[a] Yukiko Nambu,[b] Masashi Ohmae,*[a] Manabu Sugai[b] and Shunsaku Kimura[a]

Received 10th August 2018,
Accepted 2nd October 2018

DOI: 10.1039/c8ob01955j

rsc.li/obc

Immune responses against Lewis y (LY) displayed on nanocarriers at different surface densities were studied. The high surface density of LY was obtained by the A_2B-type amphiphilic polypeptides having LY at the two terminals [LY-poly(sarcosine)$_2$-*b*-(L- or D-Leu-Aib)$_6$]. The equimolar mixture of these two amphiphilic polypeptides formed interdigitated planar sheet-like molecular assemblies densely displaying LY (G4). G4 seemed to induce the anti-LY IgM upon immunization to BALB/c mice by only a single administration. However, the amount of anti-LY IgM produced was moderate and significantly less than that induced by two administrations of the other molecular assembly (G1) with the average surface density of LY at a 1/4 of that of G4. Further, the anti-LY IgM produced after two administrations of G4 lowered the avidity more than after one administration.

Published on 03 October 2018. Downloaded by Universitat de Barcelona on 1/21/2019 12:38:32 AM.

Introduction

Aberrant glycosylation occurs on tumor cells resulting in them abnormally expressing carbohydrate antigens in quality and/or quantity, which is strongly related to tumor cell biology.[1] These antigens termed tumor-associated carbohydrate antigens (TACAs) are therefore considered as good targets for the diagnosis and treatment of cancer. Particularly, cancer immunotherapy using TACAs as the antigens has attracted significant attention as cutting-edge research in the medical field.[2] TACAs are self- and T-cell-independent (TI) antigens that make it extremely difficult for the immune system to eradicate tumors with TACAs.[3] In order for such tricky but attractive TACAs to function as practical tumor antigens, they have been conjugated with highly immunogenic carriers,[4–9] or specialized carriers precisely designed to work in a T-cell-dependent (TD) manner.[10–12] These vaccine candidates, however, require multiple administrations with adjuvants, such as highly toxic Freund's complete adjuvant, and synthetic chemicals that have not been approved for use in humans to raise adequate immune responses against the target antigens. Further, the number of antigens introduced to the carriers varied depending on their synthesis lots, causing difficulty in their quality control. Multivalent presentation of TACAs can also induce an immune response, probably due to reinforced stimulation to the immune cells.[13–17] Several intriguing results have been reported in relation to the boosted antibody responses against TACAs on the basis of the concept of "self-adjuvanting vaccines".[18–20] These vaccine candidates have a unique but common molecular architecture, that is, a TACA-linker-toll-like receptor (TLR[21–23]) agonist; however, the detailed mechanism(s) for inducing potent antibody production is still unknown.

Recently, we reported the potential cancer vaccine formulation of densely TACA-presenting amphiphilic polypeptide assemblies of *ca.* 100 nm size.[24] The previously prepared molecular assemblies had interdigitated, sheet-like monolayer structures formed by equimolar amounts of the right-handed and the left-handed hydrophobic helical peptides. This system has several advantages, such as stability of the assemblies presenting dense TACAs, the flexibility of the selection and combination of the TACAs, and easy control of the density of the TACAs, which are all difficult to achieve with the traditional vaccine designs mentioned above. The TACA employed in our previous study is the Lewis y (LY) blood group antigen consisting of Fucα(1 → 2)Galβ(1 → 4)[Fucα(1 → 3)]GlcNAcβ, which is overexpressed in a variety of tumor cells.[25] Particularly in breast cancer, monoclonal antibodies (mAbs) against LY have been reported to non-competitively inhibit the interaction of

[a]*Department of Material Chemistry, Graduate School of Engineering, Kyoto University, Kyoto Daigaku-Katsura, Nishikyo-ku, Kyoto 615-8510, Japan. E-mail: ohmae.masashi.4n@kyoto-u.ac.jp*
[b]*Division of Molecular Genetics, Department of Biochemistry and Bioinformative Sciences, School of Medicine, University of Fukui, 23-3 Matsuokashimoaizuki, Eiheiji-cho, Yoshida-gun, Fukui 910-1193, Japan*

† Electronic supplementary information (ESI) available: ^{1}H and ^{13}C NMR spectra for synthesized compounds as well as additional experimental data for NTA and the AFM analysis. See DOI: 10.1039/c8ob01955j

Published on 03 October 2018. Downloaded by Universitat de Barcelona on 1/21/2019 12:38:32 AM.

the epidermal growth factor (EGF) with EGF receptors expressing LY, resulting in termination of MAPK signaling and proliferation of the tumor cell.[26] Our previous vaccine candidates could elicit anti-LY antibody in mice in a density-dependent manner of LY by using nanocarriers with planar-sheet morphology. In this study, we aimed to provoke more effective anti-LY antibody production using the exceedingly LY-presenting nanocarriers.

Results and discussion

Design and synthesis of novel amphiphilic polypeptides for the vaccine candidates with high LY density

In order to increase the surface density of LY on the nanosheet to more than that in the previous report, we newly designed two kinds of amphiphilic polypeptides with two hydrophilic chains carrying LY in each terminal with one hydrophobic helical peptide, that is, so-called A_2B-type amphiphilic polypeptides (Fig. 1). The hydrophilic block is composed of poly(sarcosine) with LY at the terminal, and the hydrophobic one is either (L-leucine-α-aminoisobutylic acid)$_6$ [(L-Leu-Aib)$_6$] or (D-Leu-Aib)$_6$; these amphiphilic polypeptides are abbreviated hereafter as 2(LY-S)-L and 2(LY-S)-D, respectively.

The structures of the hydrophilic and hydrophobic blocks are the same as those of the AB-type LY-carrying amphiphilic polypeptides previously used[23] (abbreviated as LY-S-L and LY-S-D, Fig. 1), but the new A_2B-type amphiphilic polypeptides have a branching connector between the two hydrophilic blocks and the one hydrophobic block. Therefore, 2(LY-S)-L and 2(LY-S)-D were newly synthesized according to the reactions outlined in Scheme 1.

Serinol (**1**) was coupled with mono-*t*-Bu-succinate (**2**) to obtain the dihydroxy derivative (**3**). In order to introduce amino-termini for the following poly(sarcosine) chain elongation, the two hydroxy groups in **3** were esterified with the Fmoc-protected sarcosine (**4**) to give the protected branching connector (**5**). The *t*-Bu-protection in **5** was cleaved by trifluoroacetic acid (TFA), followed by coupling with both the L-form-polypeptide (**7**)[27] and the D-form-polypeptide (**8**),[27] which gave rise to the corresponding polypeptides with the forked connector (**9** and **10**, respectively). The Fmoc protections in **9** and **10** were successfully removed by the addition of piperidine, then the secondary amino group initiated the ring-opening polyaddition of sarcosine-*N*-carboxyanhydride (Sar-NCA), followed by the terminal alkynylation through coupling with 4-pentynoic acid. After purification by Sephadex LH20 column chromatography, the forked block polypeptides with the two terminal alkynyl groups (**11** and **12**) were obtained. The average degrees of polymerization (DP) of the poly(sarcosine) blocks were determined to be 39 (**11**) and 32 (**12**) by ^{1}H NMR and MALDI-TOF MS measurements (Fig. S1 and S2†). The LY derivative (**13**)[24] was then introduced by Huisgen cycloaddition to provide the target forked block polypeptides carrying LY at both termini [2(LY-S)-L and 2(LY-S)-D].

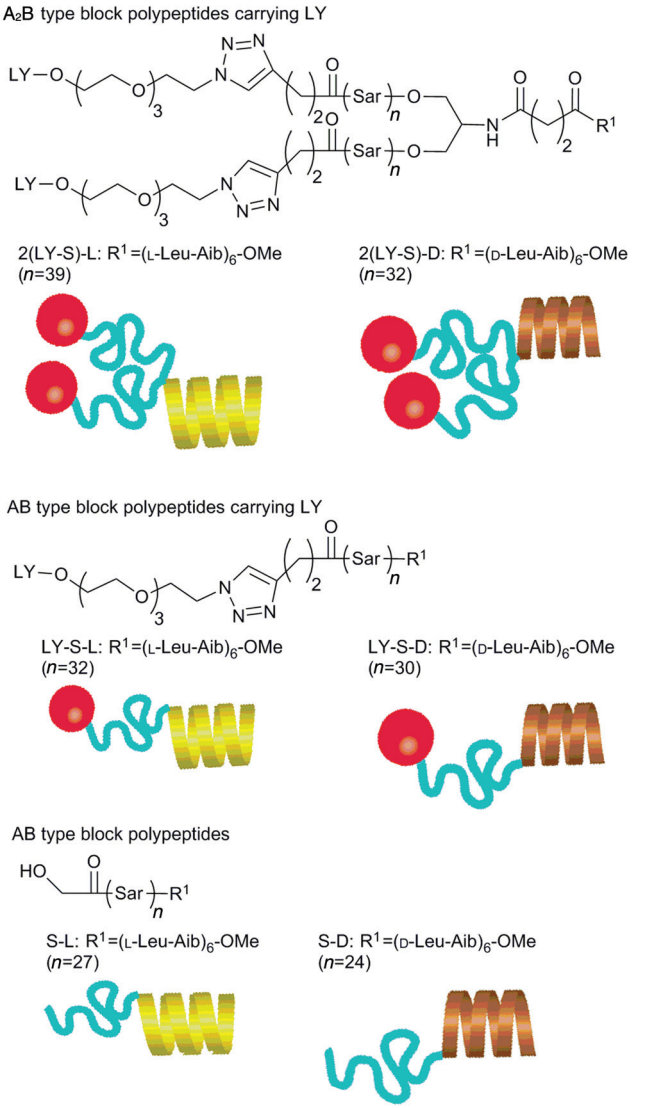

Fig. 1 Molecular designs of the amphiphilic polypeptides 2(LY-S)-L, 2(LY-S)-D, LY-S-L, LY-S-D, S-L, and S-D.

Preparation of the LY-presenting molecular assemblies using the amphiphilic polypeptides

Four kinds of molecular assemblies of nanosheets displaying LY (G1–G4) at different surface densities were prepared in addition to the nanosheet consisting of S-L and S-D without LY (G0) as a control[28] (Table 1). All the molecular assemblies have been prepared using combinations of two kinds of the amphiphilic polypeptides of the opposite chirality in the hydrophobic helical blocks at a mixing ratio of 1/1 (mol/mol). G0 has no LY, but the other assemblies are designed to have the surface LY as follows: G1 with 100% LY (the AB-type amphiphilic polypeptide protruding one LY group) only on one face (the same as that previously reported[24]), G2 with 100% LY on both faces, G3 with 200% LY (the A_2B-type amphiphilic polypeptide protruding two LY groups) on one face and 100% LY on the other, and G4 with 200% LY on both faces.

 This journal is © The Royal Society of Chemistry 2018

Published on 03 October 2018. Downloaded by Universitat de Barcelona on 1/21/2019 12:38:32 AM.

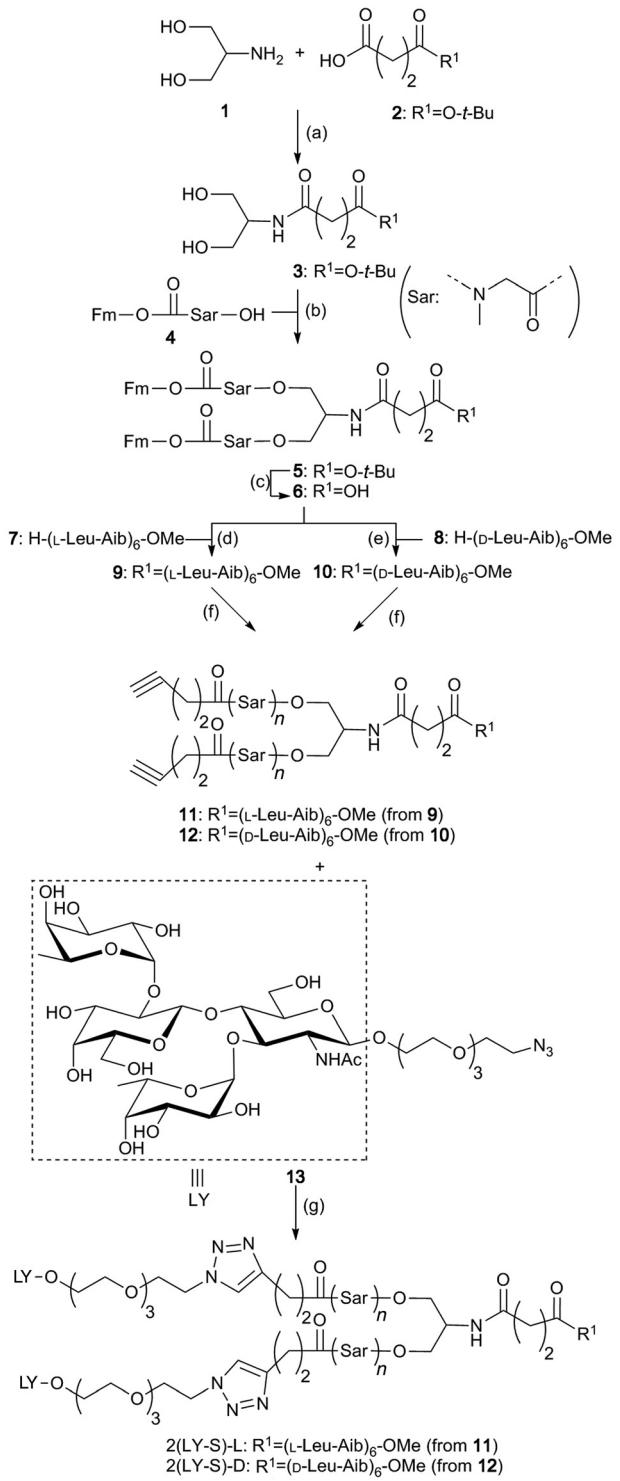

Scheme 1 Synthesis of 2(LY-S)-L and 2(LY-S)-D: (a) (1) DMT-MM, EtOH/DMF, r.t. 6 h, 95%, (b) Fmoc-sarcosine, DCC, DMAP, CH_2Cl_2/DMF, r.t. 17 h, 11%, (c) TFA, $CHCl_3$, 2 h, 83%, (d) HATU, HOAt, DIEA, DMF, 7, r.t., 12 h, 65%, (e) HATU, HOAt, DIEA, DMF, **8**, r.t., 15 h, 64%, (f) (1) piperidine, CH_3CN/CH_2Cl_2, 0 °C, (2) sarcosine-NCA, DMF, r.t., overnight, (3) 4-pentynoic acid, HATU, HOAt, DIEA, DMF, r.t., overnight, 84% (**11**), 50% (**12**), (g) Cu(I)OAc, DMF, 40 °C, 31 h, 31% [2(LY-S)-L], 39 h, 90% [2(LY-S)-D]. DIEA: *N*,*N*-diisopropylethylamine, DMT-MM: 4-(4,6-dimethoxy-1,3,5-triazin-2-yl)-4-methylmorpholinium chloride, HATU: 1-[bis(dimethylamino)methylene]-1*H*-1,2,3-triazolo[4,5-*b*]pyridinium 3-oxid hexafluorophosphate.

These molecular assemblies were filtered through a 0.8 μm cellulose acetate membrane before use.

Physical characterization of the molecular assemblies was carried out by nanoparticle tracking analysis[29] (NTA) for the size and particle concentrations and conventional DLS analyses for the size and polydispersity index. The sizes of all the molecular assemblies determined by the NTA analysis were in the range from *ca.* 80 to 190 nm. Both G0 and G1 were 160–190 nm in size with higher particle concentrations. These results indicate that stable molecular assemblies were formed with G0 and G1. The size of G2 was the smallest among all the molecular assemblies, suggesting that LY-S-L and LY-S-D are difficult to assemble with each other, probably because of too many hydrophilic LY groups existing in the AB-type molecular assembly. In fact, small particles around *ca.* 10 nm were detected during the NTA analysis of G2 (Fig. S3c and Fig. S6(b)†-red line). The particle concentration of G3 was the lowest, but the small particles existing in G2 were not detected (Fig. S3d†). The low particle concentration of *ca.* 150 nm in G3 suggests that the nanosheet was not obtained from a mixture of 2(LY-S)-L and LY-S-D, resulting in a lack of control of the surface design of the one with 200% LY and the other with 100% LY. This is probably owing to the large difference in the molecular shapes between 2 (LY-S)-L and LY-S-D, where the former is predicted to be planar-like, and the latter to be rod-like.[30] The cone-like polypeptide tended to self-assemble into a wormlike micelle while the rod-like polypeptide self-assembled into a polymeric micelle. Therefore, G3 was excluded from the following assays.

Morphology observations of the assemblies

Morphology observations of the molecular assemblies G0–G2 and G4 were carried out by using transmission electron microscopy (TEM) and atomic force microscopy in liquid (AFM, Fig. 2). The morphology of G0 with no LY moiety (control) was consistent with that reported previously,[28] that is, a planar sheet-like shape with *ca.* 10 nm thickness, which indicates the formation of the interdigitated monolayer assemblies (Fig. S4†). Similarly, G1 formed a planar-sheet monolayer with *ca.* 10 nm thickness (Fig. 2a). G2 also showed molecular assemblies with a flat region in the AFM image, however, with 5 nm thickness (Fig. 2b), suggesting that G2 self-assembled into nanosheets with a loose molecular packing structure, which allowed the chain-bending conformation in the poly (sarcosine) layer to make the thickness thin.[31] The chain-bending may prevent the LY groups from exposure to the outside. G4 was found to self-assemble into a planar sheet-like morphology with a little larger thickness (*ca.* 15 nm) (Fig. 2c). The large thickness should be owing to the dense molecular packing leading to the extended conformation of poly(sarcosine) blocks. G4, therefore, displays LY groups densely on the surface. It is notable that the combination of 2(LY-S)-L and 2 (LY-S)-D provided nanosheets that were more stable than the combination of LY-S-L and LY-S-D, even though the former combination is more hydrophilic than the latter. The planar-

Published on 03 October 2018. Downloaded by Universitat de Barcelona on 1/21/2019 12:38:32 AM.

like molecular shape of 2(LY-S)-L and 2(LY-S)-D was pointed out to favor molecular stacking to grow into a worm-like micelle.[30] The planar-like molecular shape is therefore the reason for the formation of the stable nanosheets of G4. Thus, both G1 and G4 have similar planar sheet-like morphologies, whereas G4 displays 4-fold more LY on the surface compared to G1, as we designed.

Immune responses

The molecular assemblies of G0–G2 and G4 were administered intraperitoneally to BALB/c mice (8-week-old) in addition to the monophosphoryl lipid A (MPL) adjuvant according to the time schedule including two administrations (Fig. 3a). After the first administration (at day 7, Fig. 3b), the anti-LY IgM was

Table 1 Molecular assemblies prepared from the combination of the amphiphilic polypeptides

Sample	Contents[a]	LY-display[b] /%/%	NTA		DLS	
			Size/nm	Conc. ($\times 10^{-11}$)/particles per mL	Size/nm	PDI
G0	S-L/S-D	0/0	189	3.26	198	0.07
G1	LY-S-L/S-D	100/0	156	7.04	104	0.13
G2	LY-S-L/LY-S-D	100/100	78	1.96	74	0.17
G3	2(LY-S)-L/LY-S-D	200/100	148	0.77	119	0.25
G4	2(LY-S)-L/2(LY-S)-D	200/200	129	1.92	92	0.15

[a] Molar ratio is 1 : 1. An aliquot of ethanol solution of the mixed amphiphiles was injected into saline. [b] Designed surface density of LY.

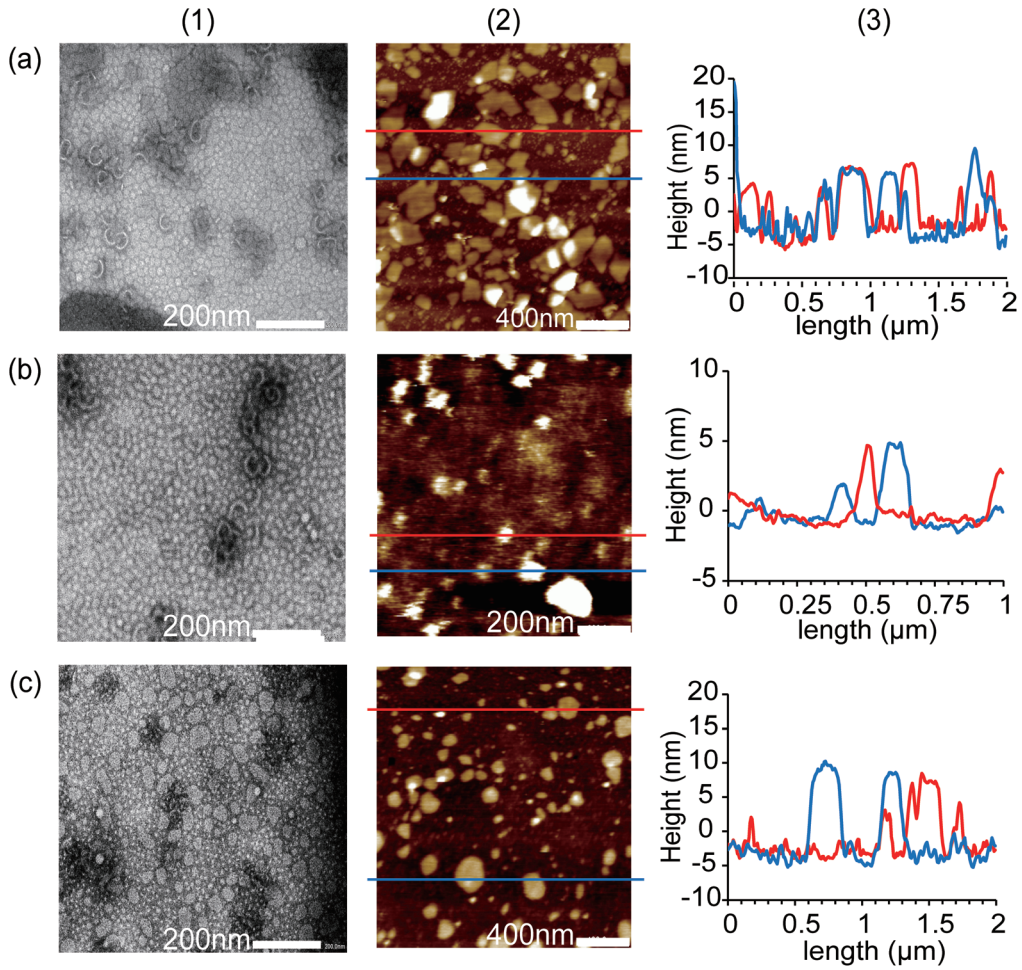

Fig. 2 Morphology observations of the assemblies (a) G1, (b) G2 and (c) G4. The columns show (1) the TEM images, (2) the AFM images and (3) the height traces of the assemblies. The AFM images were recorded on an APTES-modified Si-wafer in water. The height profiles were obtained by tracing along the red and the blue lines.

 This journal is © The Royal Society of Chemistry 2018

Published on 03 October 2018. Downloaded by Universitat de Barcelona on 1/21/2019 12:38:32 AM.

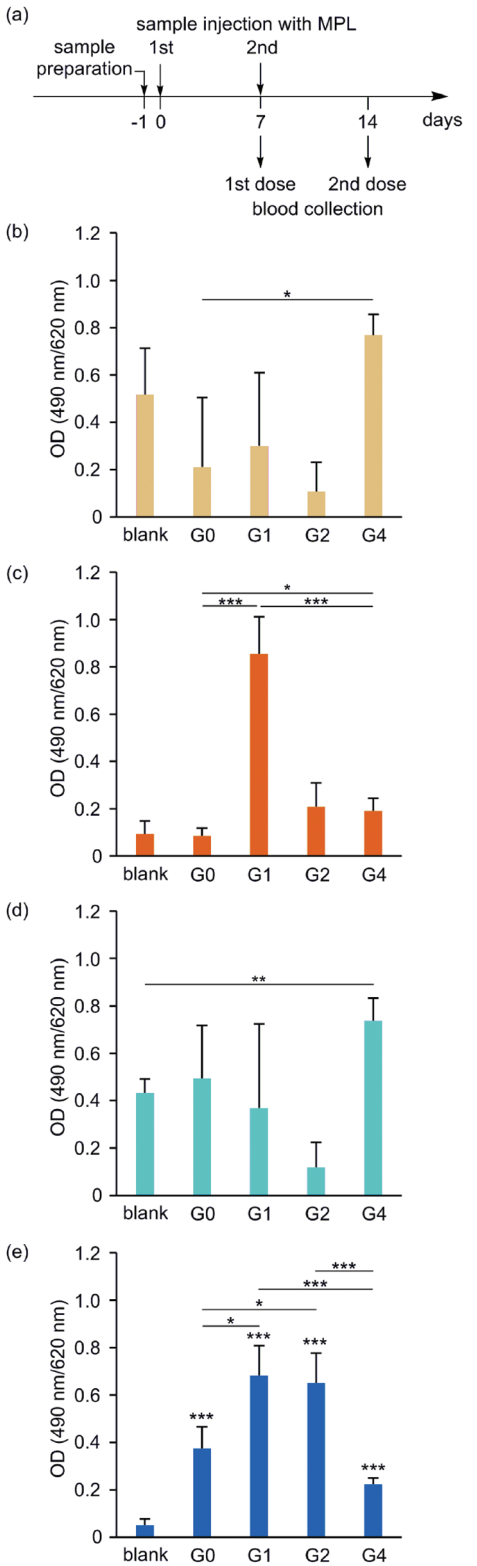

Fig. 3 Immune responses against the assemblies G0–G2 and G4: (a) The time schedules for the experiments, (b) IgM amounts by ELISA against anti-LY at day 7 and (c) day 14, and (d) anti-poly(sarcosine) at day 7 and (e) day 14. The *p*-value: $*p < 0.05$, $**p < 0.01$, $***p < 0.005$.

significantly produced only by G4, but not G1 and G2. After the second administration (at day 14, Fig. 3c), the anti-LY IgM was produced most effectively by G1, but G2 was insignificant. Unexpectedly, G4 was not as effective at triggering the immune response compared to G0.

From the structural viewpoint of the molecular assemblies, the poly(sarcosine) block also triggered the immune response in addition to the LY moiety.[32,33] After the first administration, only G4 moderately produced the anti-poly(sarcosine) IgM, but others showed no significant production of anti-poly(sarcosine) IgM (Fig. 3d). This result is consistent with our previous report that poly(sarcosine) displayed on nanosheets induced less immune responses than that on polymeric micelles.[34] In contrast, after two administrations the anti-poly(sarcosine) IgM was significantly produced by all the molecular assemblies (Fig. 3e). The IgM production increased in the order of G4 < G0 < G2 ~ G1. Taken together, G1 was the most effective in production of anti-LY IgM and anti-poly(sarcosine) IgM after two administrations. On the other hand, G4 instantly triggered the production of both anti-LY and poly(sarcosine) IgMs, but the responses became moderate after two administrations.

This suppressive immunity might have been caused *via* so-called "carrier-induced epitope suppression",[35] or *via* regulatory B cell (Breg) generation.[36] Recently, suppressive immunity against excess immune response has been reported, which can be induced by Bregs. Bregs are believed to derive from various B cell subsets including mature B cells and plasmablasts,[37] and are known to actively secrete interleukin-10 (IL-10), which is an immune suppressive cytokines.[38] B cell activation by the B cell receptors (BCR) with costimulation through toll-like receptor 4 (TLR4) can induce Breg generation.[39] In the present study, the combined use of the molecular assemblies with the MPL adjuvant, which is a TLR4 agonist,[40] therefore, could generate Bregs. Thus, we suppose that the unexpected immune suppression against G4 was caused through the generation of Bregs, although the detailed mechanism is still unknown.

There are some reports that a linker moiety attached to a carrier protein in the TACA vaccine had an effect on the production of antibody against TACA.[41,42] It is possible that the linker/spacer region in the amphiphilic polypeptide could lead to the immune suppression; however, the IgMs against other parts of the amphiphilic polypeptides, such as the oligo-ethylene oxide linker containing the triazole moiety and the helix peptide (L), were not detected at all (Fig. S8†). Furthermore, other classes of antibodies than IgM were not detected in any serum samples (Fig. S9†).

Specificity of the anti-LY IgMs

Specificity of anti-LY IgM was studied by competitive inhibition assay using ELISA on LY-L coating plates (Fig. 4). Free LY [Fucα(1 → 2)Galβ(1 → 4)[Fucα(1 → 3)]GlcNAc-OH] and G1 were employed as the inhibitors. Free LY could weakly inhibit the binding of the IgM induced after the two administrations of G1, indicating that the epitope of the anti-LY IgM consists

Published on 03 October 2018. Downloaded by Universitat de Barcelona on 1/21/2019 12:38:32 AM.

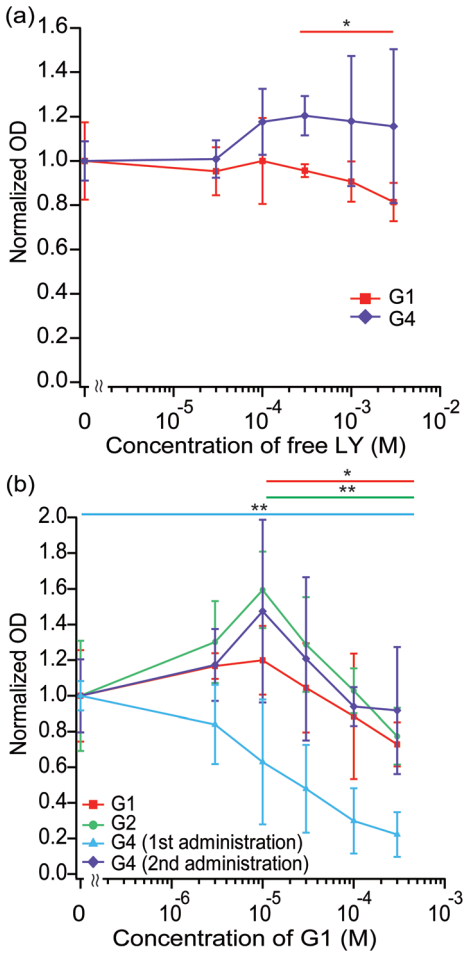

Fig. 4 Competitive inhibition assay of the anti-LY IgMs by ELISA on LY-L-coating plate with (a) free LY in the sera of the G1 (2 administrations) and the G4 (2 administrations) assemblies, and with (b) the G1 assemblies in the sera of the G1 (2 administrations), the G2 (2 administrations) and the G4 (1 and 2 administrations) assemblies. The *p*-value: $*p < 0.05$, $**p < 0.01$.

of LY. On the other hand, the anti-LY IgM assay after the two administrations of G4 was not inhibited by free LY (Fig. 4a). When G1 was used as an inhibitor, IgM in the serum after the two administrations of G1 or G2 was inhibited to adsorb to the ELISA plate at a lower concentration of G1 than that of free LY because of the multivalency of LY on the surface of the self-assemblies. Notably, G1 showed an inhibitory effect against anti-LY IgM obtained by one administration of G4, but the inhibition became less with the serum after two administrations of G4 (Fig. 4b). Accordingly, the IgM species should be different between one and two administrations. The major epitope of IgM after the two administrations of G4 differs from LY, however, the detailed mechanism remains to be solved.

In the competitive inhibition assay, IgM produced by one administration of G4 was inhibited by the addition of G1 similarly to IgM after the two administrations of G1. These suggest that IgMs have similar avidity between on administration of G4 and two administrations of G1. This observation also points out the instant response by G4 as described above.

Conclusion

Two kinds of the A_2B-type block polypeptides with LY at both hydrophilic termini [2(LY-S)-L and 2(LY-S)-D] have been successfully synthesized for the first time. These two polypeptides have the chiral blocks of L and D polypeptides, which could form the interdigitated planar sheet-like monolayer (G4) when they were mixed in equimolar amounts in saline. G4, to the best of our knowledge, has the highest surface density of LY among those prepared as cancer vaccine candidates to date. The G4 assemblies could induce the production of the IgM specific for LY through only one administration. This instant production of anti-LY IgM by G4 is remarkable, but the immune response became moderate after two administrations accompanying changes in IgM specificity. The super high surface density is therefore considered not to be suitable to trigger the immune response under the condition of multiple doses, for instance, of the booster effect. Further, the A_2B-type molecular shape contributed to the stabilization of nanosheets, but resulted in modulation in the immune responses. It is interesting to know that the immune responses *via* B cells are sensitively affected by geometrical arrangements of LY groups on nanocarriers. In the future, for inducing a more effective immune response to TACAs, we will prepare some vaccine candidates with a set of TACAs and T cell epitopes as components of the amphiphiles. These molecular architectures could induce immunological memory and antibody class switching. We will also examine adjuvants other than MPL for better vaccine formulation.

Experimental

General

Anhydrous MeOH and CH_2Cl_2 were purchased from Wako Pure Chemical Industries, Ltd. Other chemicals were purchased from commercial sources and were used without further purification. Silica gel 60 (spherical, neutral) for column chromatography was purchased from Nacalai Tesque. Transmission electron micrography (TEM) images were taken using a JEM-2000EX II or JEM-1400 (JEOL Ltd, Japan). Dynamic light scattering (DLS) measurements were taken using a DLS-8000KS (Photal Otsuka Electronics). The concentration of the molecular assembly was determined by nanoparticle tracking analysis (NTA 3.2 Dev Build 3.2.16) using NANOSIGHT LM10 (Malvern).[29] Atomic force microscopy (AFM) images were obtained using a MultiMode 8-HR (Bruker). TLC was carried out on silica gel 60 F254 (Merck). NMR spectra were recorded on a Bruker DPX400 spectrometer. HRMS (ESI-MS analysis) spectra were obtained on an Exactive Plus spectrometer (Thermo Fischer Scientific). MALDI-TOF mass spectra were recorded on an Autoflex III plus (Bruker)

 This journal is © The Royal Society of Chemistry 2018

Published on 03 October 2018. Downloaded by Universitat de Barcelona on 1/21/2019 12:38:32 AM.

spectrometer using super-DHB (Sigma-Aldrich) or α-cyano-4-hydroxycinnamic acid (CHCA; Sigma-Aldrich) as the matrix. Purification by silica gel column chromatography was carried out by elution of a column with a stepwise gradient elution procedure or using a CombiFlash Rf 75 system with a linear gradient elution procedure using standard conditions. Chemical reactions were monitored by TLC visualized by immersion in an appropriate stain (10% H_2SO_4, 500 mL; $H_3(PMo_{12}O_{40})nH_2O$, 12.5 g; $Ce(SO_4)_2nH_2O$, 5 g, or 5% ninhydrin in ethanol) followed by heating.

Preparation of peptide assemblies

An equimolar mixture of the polypeptides solution (1 mg in 20 μL EtOH) was injected into saline (1 mg/1 mL; Otsuka Pharmaceutical Co., Ltd), and kept stirring at 4 °C for 30 min. Each prepared sample was filtered using a 0.80 μm cellulose acetate syringe filter (Tokyo Roshi).

Transmission electron microscopy (TEM)

A drop of the molecular assembly dispersed in saline was mounted on a carbon-coated Cu grid and stained negatively with 2% uranyl acetate, followed by suction of the excess fluid with filter paper. TEM images were obtained at an accelerating voltage of 100 kV.

Dynamic light scattering (DLS)

Each prepared sample (1.0 mg in 1.0 mL saline) was filtered using a 0.80 μm cellulose acetate syringe filter (Tokyo Roshi), and then measured by DLS8000KS at 25 °C.

Substrate modification for atomic force microscopy (AFM)

A Si wafer was cleaned successively with 2% hydrofluoric acid and a piranha solution. Then, the Si wafer was treated with 1% 3-aminopropyltriethoxysilane (APTES) solution (toluene) at 60 °C for 10 min. The surface modification was confirmed to be a monolayer of APTES with a thickness of about 1 nm by AFM (data not shown).

Imaging by AFM

Topological images of the molecular assemblies were obtained in saline using a Multimode 8 AFM with Peak force QNM in an aqueous mode with a gold-coated silicon tip on a nitride cantilever (SCANASYST-FLUID+, 0.7 N m^{-1}, Bruker) on an APTES-modified Si wafer. Before measuring the images, the freshly prepared dispersion of the molecular assembly in saline was incubated in a fluid liquid cell on an APTES-modified Si wafer at room temperature for 30 min, and then the excess molecular assemblies in the fluid liquid cell were removed gently by replacing with saline using a syringe.

Nanoparticle tracking analysis (NTA)

A freshly prepared dispersion of the molecular assembly (5.0 μg mL^{-1} saline) was injected into an optical cell using a syringe. Each sample was measured three times for 1 min at room temperature under the flow of the mixture using a syringe pump. After measuring three times, the concentration of the molecular assembly was calculated according to the Stokes–Einstein equation as described below:

$$\sqrt{(x,\ y)^2} = \frac{2K_BT}{3r_h\pi\eta}$$

where K_B is the Boltzmann constant and $\sqrt{(x,\ y)^2}$ is the mean squared speed of a particle at a temperature T, in a medium of viscosity η, with a hydrodynamic radius of r_h.

ELISA assay

An 8-week-old BALB/c mouse (n = 4 per group, Japan SLC, Inc., Japan) was administered 100 μL of each sample intraperitoneally by subcutaneous injection. The blood was collected from eyegrounds at 7 and 14 days, and then the serum was obtained by centrifugation (3000 rpm, 10 min) after the blood had been left to stand at 4 °C overnight. For coating the 96-well plates, S-L was dissolved in acetonitrile, and LY-L, PEG-($_L$-Leu-Aib)$_6$-OMe and Boc-($_L$-Leu-Aib)$_6$-OMe were dissolved in MeOH. Each solution was put into a well (50 μL per well), followed by air-drying completely at 4 °C overnight. Then, the blocking buffer [2% BSA in phosphate-buffered saline (PBS)] was added (150 μL per well) followed by incubation for 2 h at room temperature. For the competitive inhibition assays, the inhibitor (free LY or G1) was added to the sera prior to incubation. All the wells were washed three times with PBS-T (PBS containing 0.05% Tween 20). The sera with serial dilution were added to the wells, incubated for 2 h at room temperature, and washed three times with PBS-T. Peroxidase-conjugated goat-anti-mouse IgM (Southern Biotech, USA), IgA (abcam, USA), IgG1 (abcam, USA), IgG2a (abcam, USA) or IgG3 (Southern Biotech, USA) in 0.1% BSA in PBS (50 μL) was added to the wells as the secondary antibody according to the protocol provided by the suppliers. After incubation for 2 h at room temperature, the wells were washed again three times with PBS-T. *o*-Phenylenediamine (0.5 mg mL^{-1}, Sigma, St Louis, MO) dissolved in 0.0003% H_2O_2–0.1 M citrate phosphate buffer (pH 5.0) was added to the wells, and the plate was kept standing at 30 °C for 10 min. 2 M H_2SO_4 aqueous solution was added to terminate the reaction, then the OD was determined by UV measurements (Thermo Scientific, MultiSkan FC Advance) at 490 nm/reference at 620 nm.

Statistical analysis

Differences between groups in antibody production and competitive inhibition assays were assessed using the t-test for independent samples (n = 3). A P value <0.05 is considered statistically significant. P < 0.05, <0.01 and <0.005 are designated by *, ** and ***, respectively.

Ethics

All of our *in vivo* animal experiments were approved by the Animal Care and Use Committee of the University of Fukui. Animals were treated humanely.

Published on 03 October 2018. Downloaded by Universitat de Barcelona on 1/21/2019 12:38:32 AM.

Synthesis

Preparation of LY-S-L, S-L, S-D and the LY derivative (13). LY-S-L, S-L, S-D and the LY derivative (**13**) were prepared according to the procedures reported previously.[24–26,43]

Butanoic acid, 4-[[2-hydroxy-1-hydroxymethylethyl]amino]-4-oxo-*tert*-buthyl ester (3). To a mixed solution of 2-amino-1,3-di-propanol (**1**: 1.0 g, 11.0 mmol) and mono-*t*-Bu-succinate (**2**: 2.9 g, 19.5 mmol) in an EtOH–dry DMF mixture (30 mL–15 mL) was added 4-(4,6-dimethoxy-1,3,5-triazin-2-yl)-4-methylmorpholinium chloride (DMT-MM) (3.6 g, 13.2 mmol) at 0 °C. After stirring at room temperature under a dry atmosphere for 9 h, the reaction mixture was concentrated under reduced pressure. The residue was purified by silica gel column chromatography eluting with $CHCl_3$/MeOH (1 : 0 to 6 : 1, v/v, R_f 75 system, linear gradient) to afford **3** (2.6 g, 10.5 μmol, 95%) as a colorless syrup. ^{1}H NMR (400 MHz, $CDCl_3$) δ (ppm) 6.90 (d, 1H J = 7.6 Hz, N*H*), 3.94–3.91 (m, 1H, $CH_2CHNHCH_2$), 3.83–3.69 (m, 4H, $CH_2CHNHCH_2$), 2.60, 2.46 (t × 2, 4H, J = 6.8 Hz, $COCH_2CH_2CO$), 1.44 (s, 9H, *t*-Bu). ^{13}C NMR (100 MHz, $CDCl_3$) δ (ppm) 172.90, 172.67 (C=O), 81.15 (*t*-Bu), 62.31 ($CH_2CH(NH)CH_2$), 52.68 ($CH_2CH(NH)CH_2$), 31.10, 30.80 ($COCH_2CH_2CO$), 26.04 (*t*-Bu). HRMS (ESI) m/z: $[M + Na]^+$, calcd for $C_{11}H_{21}NNaO_5$ 270.1317; found, 270.1309.

Synthesis of compound 5. To a solution of **3** (2.6 g, 10.5 mmol) and Fmoc-Sar-OH (**4**: 7.8 g, 25.2 mmol) in dry CH_2Cl_2–dry DMF (20 mL–20 mL) was added *N*,*N*′-dicyclohexylcarbodiimide (DCC; 8.6 g, 42.1 mmol) and 4-dimethylaminopyridine (DMAP; 0.6 g, 5.26 mmol) at 0 °C. After stirring at room temperature under an N_2 atmosphere for 17 h, the reaction mixture was concentrated under reduced pressure. The residue was purified by silica gel column chromatography eluting with $CHCl_3$/MeOH (1 : 0 to 6 : 1, v/v, R_f 75 system, linear gradient) and then *n*-hexane/EtOAc (1 : 0 to 0 : 1, v/v, R_f 75 system, linear gradient) to afford **5** (0.94 g, 1.13 μmol, 11%) as a white amorphous powder. ^{1}H NMR (400 MHz, $CDCl_3$) δ (ppm) 7.78–7.29 (m, 16H, aromatic group of Fmoc group), 6.29–6.15 (m, 1H, N*H*), 4.49–3.91 (m, 15H, $CHCH_2CO$ of Fmoc group, CH_2 of Sar, $CH_2CHNHCH_2$, $CH_2CHNHCH_2$), 3.07–2.97 (m, 6H, NCH_3 of Sar), 2.60, (m, 2H, $COCH_2CH_2CO$), 2.46 (m, 2H, $COCH_2CH_2CO$), 1.42 (s, 9H, *t*-Bu). ^{13}C NMR (100 MHz, $CDCl_3$) δ (ppm) 172.47, 172.17, 169.64, 157.16 (carbonyl carbons of Fmoc and succinate), 144.17, 141.62, 128.05, 127.42, 125.36, 125.15, 120.32 (aromatic groups of Fmoc), 81.10 (*t*-Bu), 68.33, 67.98, 63.52, 51.24, 51.19, 50.51, 47.42 ($CHCH_2CO$ of Fmoc group, CH_2 of Sar, $CH_2CHNHCH_2$), 36.30, 36.05 (NCH_3 of Sar), 31.27, 30.83 ($COCH_2CH_2CO$), 28.38 (*t*-Bu). HRMS (ESI) m/z: $[M + Na]^+$, calcd for $C_{47}H_{51}N_3NaO_{11}$ 856.3421; found, 856.3424.

Method for removal of *t*-butyl ester group in compound 5. To a solution of **5** in $CHCl_3$ (0.5 mL) was added trifluoroacetic acid (TFA; 2.0 mL) and anisole (0.2 mL). After stirring at room temperature for 2 h, the reaction mixture was concentrated under reduced pressure. Completion of the reaction was determined by ^{1}H NMR and ESI-MS. The residue was washed with diisopropyl ether and dried under reduced pressure to give **6** (145 mg, 0.186 mmol, 83%). ^{1}H NMR (400 MHz, $CDCl_3$) δ (ppm) 7.75–7.29 (m, 16H, aromatic group of fmoc group), 6.68–6.55 (1H J = 4.8 Hz, N*H*), 4.50–3.87 (m, 15H, $CHCH_2CO$ of Fmoc group, CH_2 of Sar, $CH_2CHNHCH_2$, $CH_2CHNHCH_2$), 3.03–2.98 (m, 6H, NCH_3 of Sar), 2.60, (m, 2H, $COCH_2CH_2CO$), 2.46 (m, 2H, $COCH_2CH_2CO$), HRMS (ESI) m/z: $[M + Na]^+$, calcd for $C_{43}H_{43}N_3NaO_{11}$ 800.2795; found, 800.2781.

Synthesis of compound 9. To a mixture of **6** (65 mg, 83.5 μmol) and H-($_L$LeuAib)$_6$-OMe (**7**: 68 mg, 55.7 μmol) in dry CH_2Cl_2–dry DMF (2.0 mL–2.0 mL) was added 2-(1-*H*-7-azabenzotriazol-1-yl)-1,1,3,3-tetramethyl uronium hexafluorophosphate methanaminium (HATU) (85 mg, 0.223 mmol), 1-hydroxy-7-azabenzotriazole (HOAT) (30 mg, 0.223 mmol) and diisopropyl ethyl amine (DIEA) (105 μL, 0.557 mmol) at 0 °C. After stirring at room temperature under an Ar atmosphere for 12 h, the reaction mixture was concentrated under reduced pressure. The residue was purified by silica gel column chromatography eluting with $CHCl_3$/MeOH (1 : 0 to 6 : 1, v/v, R_f 75 system, linear gradient), and then Sephadex LH-20 eluting with $CHCl_3$/MeOH (1 : 1, v/v) to afford **9** (72 mg, 36.3 μmol, 65%) as a white amorphous powder. ^{1}H NMR (400 MHz, MeOH-d_4) δ (ppm) 8.12–7.24 (m, 28H, aromatic group of fmoc group, amide), 4.42–3.86 (m, 21H, LeuCαH, $CHCH_2CO$ of Fmoc group, CH_2 of Sar, $CH_2CHNHCH_2$, $CH_2CHNHCH_2$), 2.98–2.87 (m, 6H, NCH_3 of Sar), 2.80–2.76 (m, 1H, $COCH_2CH_2CO$), 2.47–2.32 (m, 3H, $COCH_2CH_2CO$), 1.8–1.3 (m, 54H, $LeuCH_2$, LeuCγH, $AibCH_3$), 0.88–0.74 (m, 36H, Leu $(CH_3)_2$). HRMS (MALDI-TOF MS, CHCA) m/z: $[M + Na]^+$, calcd for $C_{104}H_{153}N_{15}NaO_{23}$ 2004.120; found, 2004.893.

Synthesis of compound 10. To a solution of **6** (110 mg, 141.2 μmol) and H-($_D$LeuAib)$_6$-OMe (**8**: 115 mg, 94.1 μmol) in dry DMF (5.0 mL) was added HATU (143 mg, 0.377 mmol), HOAT (48 mg, 0.377 mmol) and DIEA (172 μL, 0.941 mmol) at 0 °C. After stirring at room temperature under an Ar atmosphere for 15 h, the reaction mixture was concentrated under reduced pressure. The residue was diluted with $CHCl_3$, and washed successively with 4% aq. $KHSO_4$, saturated aq. $NaHCO_3$, and brine. The organic layer was dried over Na_2SO_4, filtered through a bed of diatomaceous earth (Celite), and concentrated under reduced pressure. The residue was purified by Sephadex LH-20 eluting with $CHCl_3$/MeOH (1 : 1, v/v) to afford **10** (180 mg, 90.8 μmol, 64%) as a white amorphous powder. ^{1}H NMR (400 MHz, $CDCl_3$, TMS) δ (ppm) 7.89–7.29 (m, 28H, aromatic group of fmoc group, amide), 4.41–3.93 (m, 21H, LeuCαH, $CHCH_2CO$ of Fmoc group, CH_2 of Sar, $CH_2CHNHCH_2$, $CH_2CHNHCH_2$), 3.65 (s, 3H, OCH_3), 3.09–2.99 (m, 6H, NCH_3 of Sar), 2.71–2.32 (m, 4H, $COCH_2CH_2CO$), 1.84–1.22 (m, 54H, $LeuCH_2$, LeuCγH, $AibCH_3$), 0.89–0.78 (m, 36H, Leu$(CH_3)_2$).HRMS (MALDI-TOF MS, CHCA) m/z: $[M + Na]^+$, calcd for $C_{104}H_{153}N_{15}NaO_{23}$ 2004.120; found, 2004.113.

Synthesis of compound 11. To a solution of **9** (44 mg, 22.2 μmol) in anhydrous CH_2Cl_2 (800 μL) was added 3 M piperidine in anhydrous CH_2Cl_2 (800 μL) at 0 °C. After stirring for 30 min at 0 °C, the reaction mixture was poured into petroleum ether, and the formed precipitate was washed with petroleum ether three times, followed by drying *in vacuo*. To a solution of the residue in DMF–CH_2Cl_2 (1.5 mL–1.5 mL) was

 This journal is © The Royal Society of Chemistry 2018

Published on 03 October 2018. Downloaded by Universitat de Barcelona on 1/21/2019 12:38:32 AM.

added Sar-NCA (150 mg, 1.46 mmol) under an Ar atmosphere. After complete consumption of Sar-NCA was confirmed, a solution of 4-pentyonic acid (12 mg, 130.4 μmol), HATU (50 mg, 130.4 μmol), HOAT (34 mg, 130.4 μmol) in anhydrous DMF (1.5 mL) and DIEA (60 μL, 326.0 μmol) was added therein at 0 °C under an Ar atmosphere. After stirring for 15 h under an Ar atmosphere, the solution was condensed, and the residue was purified by Sephadex LH20 column with MeOH as an eluent to afford **11** (107 mg, 84%). The degree of polymerization of the poly(sarcosine) block was determined to be 39 by ^{1}H NMR and MALDI-TOF MS measurements. ^{1}H NMR (400 MHz, MeOH-d_4) δ (ppm) 8.15–7.70 (m, 12H, amide), 4.56–3.96 (br, 167H, LeuCαH, SarCH_2, CH_2CHNHCH_2, CH$_2$CHNHCH$_2$), 3.61 (s, 3H, OCH_3), 3.01–2.88 (m, 238H, Sar N–CH_3), 2.65–2.24 (m, 14H, CHCH$_2$CH_2CO, COCH_2CH_2CO), 1.8–1.4 (m, 54H, LeuCH$_2$, LeuCγH, AibCH$_3$), 0.96–0.80 (m, 36H, Leu(CH_3)$_2$). HRMS (MALDI-TOF MS, DHB) m/z: [M + Na]$^+$, calcd for $C_{312}H_{521}N_{91}NaO_{97}$, 7120.863; found, 7119.821.

Synthesis of compound 12. 3 M Piperidine in anhydrous CH_2Cl_2 (800 μL) was added to a solution of **10** (48 mg, 24.2 μmol) in anhydrous CH_2Cl_2 (800 μL) at 0 °C. After stirring for 2 h at 0 °C, the reaction mixture was poured into petroleum ether, and the formed precipitate was washed with petroleum ether three times, followed by drying *in vacuo*. To a solution of the residue in DMF–CH_2Cl_2 (1.2 mL–1.2 mL) was added Sar-NCA (146 mg, 1.27 mmol) under Ar atmosphere. After complete consumption of Sar-NCA, a mixture of 4-pentyonic acid (12 mg, 0.130 mmol), HATU (50 mg, 0.13 mmol), and HOAT (34 mg, 0.130 mmol) in anhydrous DMF (1.0 mL) and DIEA (60 μL, 0.326 mmol) was added therein at 0 °C under an Ar atmosphere. After stirring overnight under an Ar atmosphere, the reaction mixture was concentrated, and then the residue was purified by Sephadex LH-20 column chromatography eluting with MeOH to afford **12** (76 mg, 12.1 μmol, 50%). The degree of polymerization of the poly(sarcosine) block was 33 as determined by the procedures described above. ^{1}H NMR (400 MHz, MeOH-d_4) δ (ppm) 8.12–7.70 (m, 12H, amide), 4.4–3.9 (br, 143H, LeuCαH, SarCH$_2$, CH_2CHNHCH_2, CH$_2$CHNHCH$_2$), 3.62 (s, 3H, OCH_3), 3.01–2.89 (m, 198H, Sar N–CH_3), 2.64–2.23 (m, 14H, CHCH$_2$CH_2CO, COCH_2CH_2CO), 1.8–1.4 (m, 54H, LeuCH$_2$, LeuCγH, AibCH$_3$), 0.96–0.81 (m, 36H, Leu(CH_3)$_2$). HRMS (MALDI-TOF MS, CHCA) m/z: [M + Na]$^+$, calcd for $C_{276}H_{461}N_{79}NaO_8$, 6267.414; found, 6267.933.

Synthesis of alkyne-functionalized AB type amphiphile. According to the reported synthetic method,[27] Boc-($_D$-Leu-Aib)$_6$-OMe was obtained. The Boc group of the Boc-($_D$-Leu-Aib)$_6$-OMe (58 mg, 49.1 μmol) was removed by treatment with trifluoroacetic acid (TFA, 1.5 mL) and anisole (0.15 mL). The reaction mixture was evaporated and dried *in vacuo*. The residue was dissolved in chloroform and washed with saturated $NaHCO_3$ and saturated NaCl aqueous solutions. The organic layer was dried over anhydrous Na_2SO_4 and the solvent was removed and dried *in vacuo* to afford H-($_D$-Leu-Aib)$_6$-OMe (49 mg, 0.401 mmol). To a solution of H-($_D$-Leu-Aib)$_6$-OMe in DMF/CH_2Cl_2 (2.5 mL, 1/1, v/v) was added Sar-NCA (138 mg, 1.20 mmol) under an Ar atmosphere. After complete consumption of the Sar-NCA was confirmed, a solution of 4-pentyonic acid (12 mg, 0.120 mmol), HATU (60 mg, 0.160 mmol), and HOAT (21 mg, 0.160 mmol) in anhydrous DMF (500 μL) and DIEA (68 μL, 0.400 mmol) was added at 0 °C under Ar atmosphere to react with the N-terminal. After stirring for 24 h under Ar atmosphere, the solution was condensed, and the residue was purified by a Sephadex LH-20 column with MeOH as an eluent to afford the amphiphilic polypeptide inducing the alkyne function group (84 mg, 24.5 μmol, 61%). The degree of polymerization of the poly(sarcosine) block was determined to be 30 from the ^{1}H NMR spectrum. MALDI-TOF MS analysis also supported the degree of polymerization to be 30. ^{1}H NMR (400 MHz, MeOH-d$_4$) δ (ppm) 7.98–7.74 (m, 12H, amide), 4.4–4.0 (br, 66H, LeuCαH, SarCH$_2$), 3.65 (s, 3H, OCH_3), 3.08–2.93 (m, 90H, Sar N–CH_3), 2.68–2.66 (m, 1H, CHCH$_2$CH_2CO), 2.46–2.42 (m, 3H, CHCH_2CH_2CO), 2.26 (s, 1H, CHCH$_2$CH_2CO), 1.8–1.4 (m, 54H, LeuCH$_2$, LeuCγH, AibCH$_3$), 1.00–0.85 (m, 36H, Leu(CH_3)$_2$). HRMS (MALDI-TOF MS, CHCA) m/z: [M + Na]$^+$, calcd for $C_{156}H_{266}N_{42}NaO_{44}$, 3455.980; found, 3456.098.

Synthesis of 2(LY-S)-L. To a solution of the amphiphilic polypeptide having the alkyne functional group (**11**; 29 mg, 4.09 μmol) and **13** (12 mg, 13.7 μmol) in anhydrous DMF (1.0 mL) was added Cu(I)OAc (2 mg, 16.3 μmol). After stirring at 40 °C for 31 h, the solution was condensed, and the residue was purified by a Sephadex LH-20 column with MeOH as an eluent to afford 2(LYS)-L (11 mg, 1.2 μmol, 31%). The degree of polymerization of the poly(Sar) block was determined to be 41 by ^{1}H NMR and MALDI-TOF MS analysis. ^{1}H NMR (400 MHz, MeOH-d_4) δ (ppm) 8.07–7.71 (m, 12H, amide), 5.11 (d, 1H J = 2.8 Hz, LY-proton), 4.98 (d, 1H J = 4.0 Hz, LY-proton), 4.55–3.35 (m, 258H, LeuCαH, SarCH_2, LY-protons, LeuAibOCH_3, OCH_2CH(NH)–CH_2O), 3.1–2.9 (m, 246H, Sar N–CH$_3$), 2.6–2.2 (br, 14H, CH_2CH_2C═CH, C═OCH_2CH_2C═O), 1.91 (s, 6H, LY-NHAc), 1.8–1.5 (m, 54H, LeuCH_2, LeuCγH, AibCH_3), 1.19–1.16 (m, 12H, LY-fucose-H6), 0.96–0.80 (m, 36H, Leu (CH_3)$_2$). HRMS (MALDI-TOF MS, super DHB) m/z: [M + Na]$^+$, calcd for $C_{392}H_{661}N_{103}NaO_{145}$, 9158.7548; found, 9158.994.

Synthesis of 2(LY-S)-D. To a mixture of **12** (23 mg, 3.68 μmol) and **13** (10 mg, 11.4 μmol) in anhydrous DMF (1.0 mL) was added Cu(I)OAc (2 mg, 16.3 μmol). After stirring at 40 °C for 39 h, the mixture was condensed, and then the residue was purified by Sephadex LH-20 column chromatography eluting with MeOH to afford 2(LYS)-D (27 mg, 3.4 μmol, 90%). The degree of polymerization of the poly(Sar) block was 32, determined similarly as described above. ^{1}H NMR (400 MHz, MeOH-d$_4$) δ (ppm) 8.06–7.65 (m, 12H, amide), 5.06 (d, 1H, J = 4.0 Hz, LY-proton), 4.94–4.87 (m, 2H, LY-proton), 4.50–3.30 (m, 198H, LeuCαH, SarCH_2, LY-protons, LeuAibOCH_3, OCH_2CH(NH)–CH_2O), 3.0–2.8 (m, 192H, Sar N–CH$_3$), 2.6–2.1 (br, 14H, CH_2CH_2C═CH, C═OCH_2CH_2C═O), 1.86 (s, 6H, LY-NHAc), 1.8–1.4 (m, 54H, LeuCH_2, LeuCγH, AibCH_3), 1.14–1.11 (m, 12H, LY-fucose-H6), 0.96–0.76 (m, 36H, Leu(CH_3)$_2$). HRMS (MALDI-TOF MS, super DHB) m/z: [M + Na]$^+$, calcd for $C_{338}H_{571}N_{85}NaO_{127}$, 7879.083; found, 7879.024.

Published on 03 October 2018. Downloaded by Universitat de Barcelona on 1/21/2019 12:38:32 AM.

Synthesis of LY-S-D. To a solution of the terminal alkyne-functionalized poly(sarcosine)$_{33}$-($_D$-Leu-Aib)6-OMe (alkyne-functionalized AB type amphiphile, 31 mg, 10.9 μmol) and **13** (11 mg, 12.5 μmol) in anhydrous DMF (1.0 mL) was added Cu (I)OAc (2 mg, 16.3 μmol). After stirring at 40 °C overnight, the reaction mixture was condensed, and the residue was purified by Sephadex LH20 column chromatography eluting with MeOH to afford LY-S-D (36 mg, 8.4 μmol, 73%). The degree of polymerization of the poly(sarcosine) block was determined as described above. ^{1}H NMR (400 MHz, MeOH-d$_4$) δ (ppm) 8.07–7.71 (m, 12H, amide), 5.12 (d, 1H, J = 4.0 Hz, LY-proton), 4.99 (d, 1H, J = 4.0 Hz, LY-proton), 4.57–3.44 (m, 118H, LeuCαH, SarCH$_2$, LY-protons, OCH_3), 3.1–2.9 (m, 90H, Sar N–CH_3), 1.91 (s, 3H, LY-NHAc), 1.9–1.4 (m, 54H, LeuCH$_2$, LeuCγH, AibCH$_3$), 1.19–1.16 (m, 6H, LY-fucose-H6), 0.96–0.81 (m, 36H, Leu(CH_3)$_2$). HRMS (MALDI-TOF MS, super DHB) m/z: [M + Na]$^+$, calcd for $C_{199}H_{341}N_{49}NaO_{69}$ 4333.353; found, 4332.982.

Conflicts of interest

There are no conflicts to declare.

Acknowledgements

This study was supported by JSPS KAKENHI Grant Number JP 17J09903 for YY.

Notes and references

1 M. M. Fuster and J. D. Esko, *Nat. Rev. Cancer*, 2005, **5**, 526–542.
2 M. M. Wei, Y.-S. Wang and X.-S. Ye, *Med. Res. Rev.*, 2018, **38**, 1003–1026.
3 S. J. Danishefsky and J. R. Aleen, *Angew. Chem., Int. Ed.*, 2000, **39**, 836–863.
4 G. Ragupathi, F. Koide, P. O. Livingston, Y. S. Cho, A. Endo, Q. Wan, M. K. Spassova, S. J. Keding, J. Allen, O. Ouerfelli, R. M. Wilson and S. J. Danishefsky, *J. Am. Chem. Soc.*, 2006, **128**, 2715–2725.
5 H. Y. Chuang, C. T. Ren, C. A. Chao, C. Y. Wu, S. S. Shivatare, T. J. Cheng, C. Y. Wu and C. H. Wong, *J. Am. Chem. Soc.*, 2013, **135**, 11140–11150.
6 Y. L. Huang, J. T. Hung, S. K. Cheung, H. Y. Lee, K. C. Chu, S. T. Li, Y. C. Lin, C. T. Ren, T. J. Cheng, T. L. Hsu, A. L. Yu, C. Y. Wu and C. H. Wong, *Proc. Natl. Acad. Sci. U. S. A.*, 2013, **110**, 2517–2522.
7 S. J. Danishefsky, Y. K. Shue, M. N. Chang and C. H. Wong, *Acc. Chem. Res.*, 2015, **48**, 643–652.
8 E. Kaltgrad, S. Sen Gupta, S. Punna, C. Y. Huang, A. Chang, C. H. Wong, M. G. Finn and O. Blixt, *ChemBioChem*, 2007, **8**, 1455–1462.
9 Z. Yin, M. Comellas-Aragones, S. Chowdhury, P. Bentley, K. Kaczanowska, L. Benmohamed, J. C. Gildersleeve, M. G. Finn and X. Huang, *ACS Chem. Biol.*, 2013, **8**, 1253–1262.
10 U. Westerlind, A. Hobel, N. Gaidzik, E. Schmitt and H. Kunz, *Angew. Chem., Int. Ed.*, 2008, **47**, 7551–7556.
11 M. Shi, K. A. Kleski, K. R. Trabbic, J. P. Bourgault and P. R. Andreana, *J. Am. Chem. Soc.*, 2016, **138**, 14264–14272.
12 A. Kaiser, N. Gaidzik, T. Becker, C. Menge, K. Groh, H. Cai, Y. M. Li, B. Gerlitzki, E. Schmitt and H. Kunz, *Angew. Chem., Int. Ed.*, 2010, **49**, 3688–3692.
13 M. G. Baek and R. Roy, *Bioorg. Med. Chem.*, 2002, **10**, 11–17.
14 T. C. Shiao and R. Roy, *New J. Chem.*, 2012, **36**, 324–339.
15 D. Sames, X. T. Chen and S. J. Danishefsky, *Nature*, 1997, **389**, 587–591.
16 H. Cai, Z. Y. Sun, M. S. Chen, Y. F. Zhao, H. Kunz and Y. M. Li, *Angew. Chem., Int. Ed.*, 2014, **53**, 1699–1703.
17 B. Richichi, B. Thomas, M. Fiore, R. Bosco, H. Qureshi, C. Nativi, O. Renaudet and L. BenMohamed, *Angew. Chem., Int. Ed.*, 2014, **53**, 11917–11920.
18 Z. Zhou, M. Mondal, G. Liao and Z. Guo, *Org. Biomol. Chem.*, 2014, **12**, 3238–3245.
19 Z. Zhou, G. Liao, S. S. Mandal, S. Suryawanshi and Z. Guo, *Chem. Sci.*, 2015, **6**, 7112–7121.
20 T. Buskas, S. Ingale and G. J. Boons, *Angew. Chem., Int. Ed.*, 2005, **44**, 5985–5988.
21 S. Ingale, M. A. Wolfert, J. Gaekwad, T. Buskas and G. J. Boons, *Nat. Chem. Biol.*, 2007, **3**, 663–667.
22 S. Ingale, M. A. Wolfert, T. Buskas and G. J. Boons, *ChemBioChem*, 2009, **10**, 455–463.
23 V. Lakshminarayanan, P. Thompson, M. A. Wolfert, T. Buskas, J. M. Bradley, L. B. Pathangey, C. S. Madsen, P. A. Cohen, S. J. Gendler and G. J. Boons, *Proc. Natl. Acad. Sci. U. S. A.*, 2012, **109**, 261–266.
24 Y. Yamazaki, N. Watabe, H. Obata, E. Hara, M. Ohmae and S. Kimura, *J. Pept. Sci.*, 2017, **23**, 189–197.
25 D. H. Dube and C. R. Bertozzi, *Nat. Rev. Drug Discovery*, 2005, **4**, 477–488.
26 M. Klinger, H. Farhan, H. Just, H. Drobny, G. Himmler, H. Loibner, G. C. Mudde, M. Freissmuth and V. Sexl, *Cancer Res.*, 2004, **64**, 1087–1093.
27 T. Kanzaki, Y. Horikawa, A. Makino, J. Sugiyama and S. Kimura, *Macromol. Biosci.*, 2008, **8**, 1026–1033.
28 M. Ueda, A. Makino, T. Imai, J. Sugiyama and S. Kimura, *Chem. Commun.*, 2011, **47**, 3204–3206.
29 V. Filipe, A. Hawe and W. Jiskoot, *Pharm. Res.*, 2010, **27**, 796–810.
30 A. Makino, E. Hara, I. Hara, E. Ozeki and S. Kimura, *Langmuir*, 2014, **30**, 669–674.
31 C. J. Kim, S. Kurauchi, T. Uebayashi, A. Fujisaki and S. Kimura, *Bull. Chem. Soc. Jpn.*, 2017, **90**, 568–573.
32 E. Hara, A. Makino, K. Kurihara, F. Yamamoto, E. Ozeki and S. Kimura, *Int. Immunopharmacol.*, 2014, **14**, 261–266.
33 C. J. Kim, E. Hara, A. Shimizu, M. Sugai and S. Kimura, *J. Pharm. Sci.*, 2015, **104**, 1839–1847.
34 E. Hara, M. Ueda, C. J. Kim, A. Makino, I. Hara, E. Ozeki and S. Kimura, *J. Pept. Sci.*, 2014, **20**, 570–577.

 This journal is © The Royal Society of Chemistry 2018

Published on 03 October 2018. Downloaded by Universitat de Barcelona on 1/21/2019 12:38:32 AM.

35 L. A. Herzenberg and T. Tokushima, *J. Exp. Med.*, 1982, **155**, 1730–1740.
36 E. C. Rossoer and C. Mauri, *Immunity*, 2015, **42**, 607–612.
37 W. van de Veen, B. Stanic, O. F. Wirz, K. Jansen, A. Globinska and M. Akdis, *J. Allergy Clin. Immunol.*, 2016, **138**, 654–665.
38 R. Sabat, G. Grütz, K. Warszawska, S. Kirsch, E. Witte, K. Wolk and J. Geginat, *Cytokine Growth Factor Rev.*, 2010, **21**, 331–344.
39 K. Yanaba, J.-D. Bouaziz, T. Matsushita, T. Tubata and T. Tedder, *J. Immunol.*, 2009, **182**, 7459–7472.
40 C. B. Fox, M. riede, S. G. Reed and G. C. Ireton, in *Endotoxins: Structure, Function, and Recognition. Subcellular Biochemistry*, ed. X. Wang and P. Quinn, Springer, Dordrecht, 2010, vol. 14, pp. 303–321.
41 J. Ni, H. Song, Y. Wang, N. M. Stamatos and L. X. Wang, *Bioconjugate Chem.*, 2006, **17**, 493–500.
42 T. Buskas, Y. Li and G. J. Boons, *Chem. – Eur. J.*, 2004, **10**, 3517–3524.
43 Y. Yamazaki, K. Sezukuri, J. Takada, H. Obata, S. Kimura and M. Ohmae, *Carbohydr. Res.*, 2016, **422**, 34–44.